

# Lignin Depolymerization with Nitrate-Intercalated Hydrotalcite Catalysts

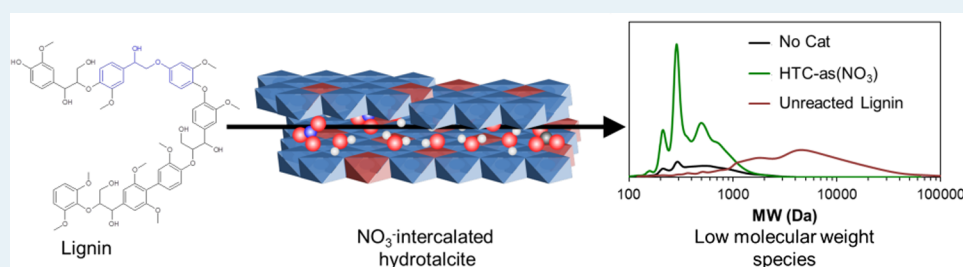
Jacob S. Kruger,<sup>†</sup> Nicholas S. Cleveland,<sup>†</sup> Shuting Zhang,<sup>†</sup> Rui Katahira,<sup>†</sup> Brenna A. Black,<sup>†</sup> Gina M. Chupka,<sup>‡</sup> Tijs Lammens,<sup>§</sup> Phillip G. Hamilton,<sup>||</sup> Mary J. Bidby,<sup>\*,†</sup> and Gregg T. Beckham<sup>\*,†</sup>

<sup>†</sup>National Bioenergy Center and <sup>‡</sup>Hydrogen and Transportation Systems Center, National Renewable Energy Laboratory, 15013 Denver West Parkway, Golden, Colorado 80401, United States

<sup>§</sup>Shell Global Solutions, Inc., Shell Technology Center, Houston, Texas 77082, United States

<sup>||</sup>Shell Global Solutions, Inc., Shell Technology Center, Amsterdam, Netherlands

## Supporting Information



**ABSTRACT:** Hydrotalcites (HTCs) exhibit multiple adjustable parameters to tune catalytic activity, including interlayer anion composition, metal hydroxide layer composition, and catalyst preparation methods. Here, we report the influence of several of these parameters on  $\beta$ -O-4 bond scission in a lignin model dimer, 2-phenoxy-1-phenethanol (PE), to yield phenol and acetophenone. We find that the presence of both basic and  $\text{NO}_3^-$  anions in the interlayer increases the catalyst activity by 2–3-fold. In contrast, other anions or transition metals do not enhance catalytic activity in comparison to blank HTC. The catalyst is not active for C–C bond cleavage on lignin model dimers and has no effect on dimers without an  $\alpha$ -OH group. Most importantly, the catalyst is highly active in the depolymerization of two process-relevant lignin substrates, producing a significant amount of low-molecular-weight aromatic species. The catalyst can be recycled until the  $\text{NO}_3^-$  anions are depleted, after which the activity can be restored by replenishing the  $\text{NO}_3^-$  reservoir and regenerating the hydrated HTC structure. These results demonstrate a route to selective lignin depolymerization in a heterogeneous system with an inexpensive, earth-abundant, commercially relevant, and easily regenerated catalyst.

**KEYWORDS:** lignin valorization, lignin nitration, layered double hydroxide, catalyst recycle, catalyst regeneration

## INTRODUCTION

Lignin is a primary component of terrestrial plant cell walls responsible for structure, defense, and water transport.<sup>1,2</sup> During lignin biosynthesis, the three primary lignin monomers (*p*-coumaryl, coniferyl, and sinapyl alcohols; Scheme 1) are connected through a variety of alkyl, aryl, and ether linkages, likely via oxidative cross-coupling reactions.<sup>3</sup> Coumaric and ferulic acid derivatives connected through ester linkages can also account for a significant fraction of lignin mass, especially in grasses.<sup>4</sup> The most common linkage in lignin, and one of the most labile, is the  $\beta$ -O-4 ether formed between the  $\beta$ -carbon of the propenyl group on one monomer and the hydroxyl oxygen and 4-carbon of a second monomer.<sup>5–7</sup> The highly aromatic structure of lignin is seemingly conducive to production of aromatic-based chemicals and high-octane fuel additives. However, the diversity of the interaromatic ring linkages presents a considerable technical barrier to the selective depolymerization of lignin. Moreover, depolymerization of natural lignin almost invariably produces a heterogeneous slate

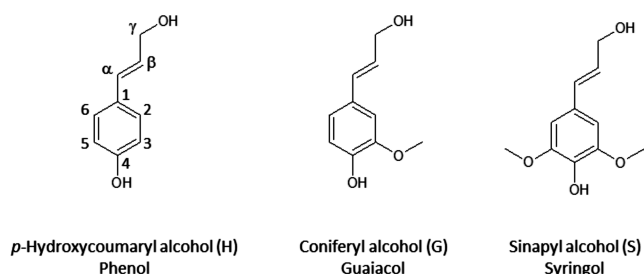
of aromatic molecules, making subsequent separation and upgrading a challenge to produce fungible chemical feedstocks in an economically viable manner.<sup>2,8</sup>

In current biorefinery designs for lignocellulosic ethanol, most byproduct lignin is slated to be used for process heat or for cofiring in power plants.<sup>9,10</sup> Going forward, however, strategies for selective lignin depolymerization will be required for upgrading lignin to higher-value end products, which is of paramount importance for advanced biofuels processes.<sup>11</sup> A number of thermochemical routes have been explored for lignin depolymerization, and low-temperature catalytic approaches that preserve the aromatic ring structure and minimize repolymerization reactions are especially promising. In this vein, several catalytic scenarios have been explored.

Received: September 15, 2015

Revised: January 7, 2016

Published: January 13, 2016

Scheme 1. Three Primary Lignin Monomers in Terrestrial Plants<sup>a</sup>

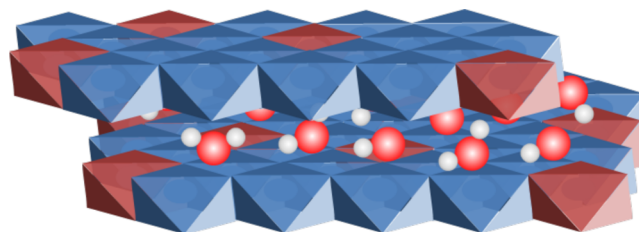
<sup>a</sup>The aromatic ring substructure (without the hydroxypropenyl group) is shown on the second line.

Heterogeneous metal catalysts and H<sub>2</sub> have been employed for many decades to simultaneously depolymerize and hydrogenate lignin via hydrogenolysis.<sup>1,12–21</sup> A few types of solid catalysts that do not require high-pressure H<sub>2</sub> for lignin depolymerization have been recently reported, including a limited number of Pd/C<sup>22</sup> and Ni/C<sup>23</sup> catalysts. In these examples, the catalysts either require addition of a hydrogen donor<sup>22,24</sup> or are hypothesized to generate hydrogen in situ from the solvent (methanol).<sup>23,25</sup> Alternatively, some heterogeneous metal oxides can catalyze lignin depolymerization in the presence of O<sub>2</sub><sup>26,27</sup> or H<sub>2</sub>O<sub>2</sub>.<sup>28,29</sup> Additionally, homogeneous metal catalysts, such as complexes and salts of Co, Mn, and Ru, are able to depolymerize lignin and lignin model compounds.<sup>1,30–41</sup> A few metal-free approaches using homogeneous oxidants have been recently developed.<sup>42,43</sup>

Finally, alkaline catalysts, such as NaOH, have been employed by Shabtai et al.,<sup>44–50</sup> Roberts et al.,<sup>51</sup> and others<sup>52,53</sup> in a “base-catalyzed depolymerization (BCD)” scheme. BCD effectively depolymerizes lignin to monomers under optimized conditions, producing more than 85 wt % yield as an oil comprised of low-molecular-weight species (monomers, dimers, trimers, and borate capping agent) when repolymerization inhibitors are added. Some solid base catalysts have been explored, including metal-doped porous metal oxides derived from calcined hydrotalcites (HTCs)<sup>54–57</sup> and metal-doped, uncalcined HTCs.<sup>58</sup> These heterogeneous base catalysts are particularly advantageous because they are derived from earth-abundant materials and do not generate high-salt-content wastewater.

HTCs belong to a class of layered double-hydroxide (LDH) minerals that exhibit activity as solid base catalysts. The structure of these catalysts is derived from a Mg(OH)<sub>2</sub> foundation, in which a plane of Mg atoms is situated between two planes of OH groups to form a brucite layer. These brucite layers are stacked, each separated by a layer of H<sub>2</sub>O molecules in the interlayer space. The Mg atoms can be substituted by other di- and trivalent atoms, such as Al. If the substituting atom is trivalent, a positive charge is introduced into the brucite layer, which is balanced by an anion in the interlayer space, as illustrated in Scheme 2. A large number of materials exist with varying types and ratios of metal atoms and charge-compensating anions.<sup>59</sup> In addition to their inherent catalytic activity as solid bases, LDH materials can serve as supports for other catalysts.<sup>60</sup>

In our previous work, we reported on a Ni-HTC catalyst that was active for β-O-4 bond cleavage in a lignin model dimer and that reduced the molecular weight of two insoluble lignin streams.<sup>58</sup> The active site in the Ni-HTC catalysts was not

Scheme 2. General Layered Double-Hydroxide Structure, with Edge-Sharing Mg(OH)<sub>6</sub> Octahedra (Blue), in Which Some of the Mg Atoms Are Replaced by Al (Red)<sup>a</sup>

<sup>a</sup>Between M(OH)<sub>2</sub> layers are H<sub>2</sub>O molecules and anions, e.g., OH<sup>−</sup>.

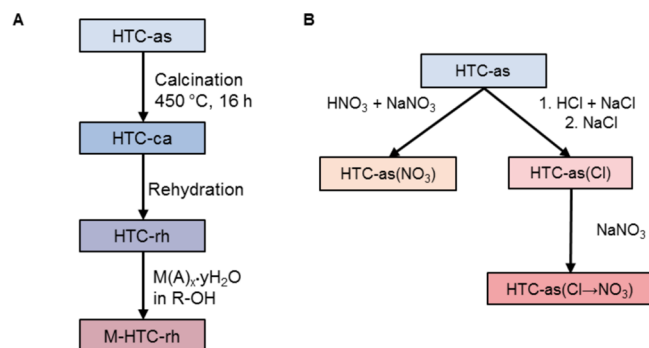
determined, but the catalyst was hypothesized to operate analogously to a homogeneous base catalyst with enhanced redox activity from the deposited Ni.<sup>58</sup> Given the need to increase catalyst activity for lignin depolymerization and to understand catalyst recyclability and regeneration, we were motivated by these initial experiments to pursue a deeper understanding of catalyst activity and reaction parameters by investigating a series of HTC catalysts prepared by different methods. For the purposes of these experiments, we have focused on commercially relevant catalyst preparation methods, such as incipient wetness deposition and ion-exchange techniques. Additionally, we focused on a lignin model compound to help elucidate the catalytic mechanism and subsequently examined the catalytic activity toward several other lignin model dimers and two process-relevant lignin streams. As described below, we find that the key component for catalytic activity is nitrate anions intercalated in the interlayer space. The nitrate anions are active even in the absence of transition metals but may benefit from neighboring basic anions, such as CO<sub>3</sub><sup>2−</sup> and OH<sup>−</sup>. The catalytic activity is heterogeneous and may result from a nitration of a benzylic hydroxyl group. These results suggest a direct means to synthesize, regenerate, and recycle nitrate-HTC catalysts for lignin depolymerization applications. Furthermore, the catalyst is active only when an α-OH group is present on the substrate, and it does not break C–C bonds. Nonetheless, the catalyst is effective for generating compounds with molecular weights indicative of monomeric and dimeric species from real lignin streams.

## RESULTS

**Metal and Precursor Screening.** The initial set of experimental studies focused on screening the activity of a set of HTC catalysts with a model lignin dimer. To explore the generality of the activity previously observed with Ni-HTC catalysts,<sup>58</sup> we conducted a survey of metal-loaded HTC-rh catalysts, varying the transition metal, metal oxidation state, and precursor salt. To gain further understanding of the roles of the metals and anions, we also explored a series of metal-free, ion-exchanged HTC as catalysts. The general preparation procedure for these catalysts is shown in Scheme 3 (as = as-synthesized, with CO<sub>3</sub><sup>2−</sup> anions; ca = calcined, mixed-oxide form, without brucite layers or interlayer anions; rh = rehydrated, with OH<sup>−</sup> anions). Details of the materials used in these experiments and methods for model compound and catalyst syntheses are given in the Experimental Section and in the Supporting Information.

The catalysts were screened in the conversion of a lignin model compound, 2-phenoxy-1-phenethanol (PE), to phenol,

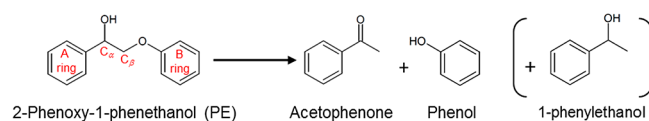
**Scheme 3. Catalyst Preparation Diagram and Naming Conventions for (A) M-HTC-rh Catalysts<sup>a</sup> and (B) Ion-Exchanged HTC Catalysts**



<sup>a</sup>For  $M(A)_x \cdot yH_2O$  in R-OH, M is a generic metal, A is a generic anion,  $x = 2, 3, 0 \leq y \leq 6$ , and  $R = CH_3CH_2, CH_3, H$ .

acetophenone, and 1-phenylethanol via  $\beta$ -O-4 bond cleavage, as shown in Scheme 4. In all cases, the reaction solvent is methyl isobutyl ketone, MIBK. Error bars in all figures represent the standard deviation of at least two replicate experiments.

**Scheme 4. Reaction of Lignin Model Compound 2-Phenoxy-1-phenethanol (PE) to Phenol, Acetophenone, and 1-Phenylethanol<sup>a</sup>**



<sup>a</sup>The A and B ring and inter-ring carbon labeling convention for lignin model dimers is shown for PE.

The results of the metal precursor screening are shown in Figure 1A, represented by phenol yield. PE conversion and acetophenone yield show similar trends (Figure S1 in the Supporting Information). These results demonstrate that, regardless of metal, all catalysts prepared from nitrate precursor salts exhibit high activity, whereas those prepared from chloride salts are no more active, or in some instances are less active, than the blank HTC-rh.

To evaluate the impact that the salt precursor has on the overall catalyst activity and gain insight into whether the nitrate salts were unique in their high activity, we prepared a series of Ni-HTC-rh catalysts from acetate, formate, and sulfate precursors. As summarized in Figure 1B, the other precursor salts also produce catalysts that are no more active, or are less active, than the blank HTC-rh. However, a metal-free, ion-exchanged HTC-as, in which the  $CO_3^{2-}$  anions were replaced by  $OH^-$  and  $NO_3^-$  anions (HTC-as( $NO_3$ )), is as active as the Ni-loaded catalyst. Characterization of these catalysts by XRD shows unique structural changes in the catalysts prepared from nitrate precursors. In particular, catalysts prepared from nitrate precursors display additional peaks at  $2\theta = 20, 38, 43^\circ$  (Figure 1C), which is characteristic of HTC domains with intercalated  $NO_3^-$  ions.<sup>61,62</sup>

These results demonstrate that a nitrate precursor is key to enhancing catalyst activity beyond blank HTC. However, retention of some basic anions appears to be beneficial for the desired reaction. We prepared a fully nitrate exchanged catalyst (HTC-as(Cl $\rightarrow$ NO<sub>3</sub>)), with no significant XRD peak for basic

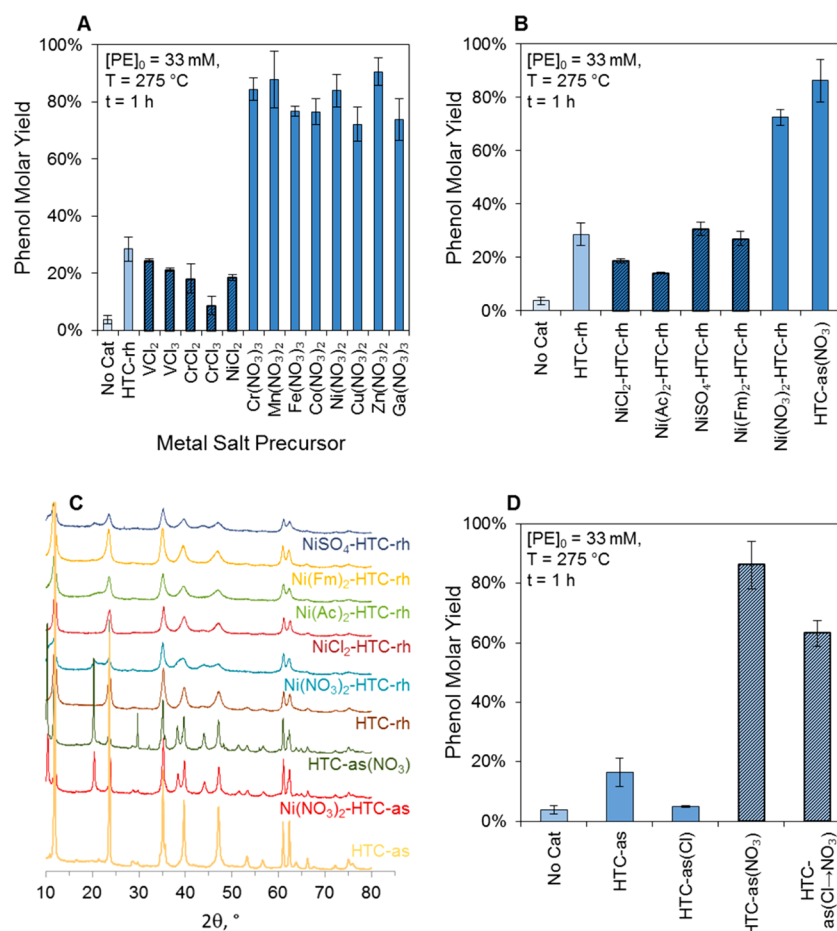
anions (Figure S2 in the Supporting Information), which showed a moderate decrease in phenol yield in comparison to the partially exchanged HTC-as( $NO_3$ ), as shown in Figure 1D. The latter catalyst still shows relatively high activity in comparison to HTC-rh and HTC-as, likely due to “XRD-invisible” basic anions still present in nitrate-dominated catalyst domains.<sup>62</sup> Indeed, benzoic acid titration of the nitrate ion-exchanged catalysts shows a slightly elevated content of basic sites relative to HTC-as (Table S1 in the Supporting Information).

Remarkably, the difference in basic site strength between Ni-HTC-as (with carbonates as basic anions) and hydroxide-form Ni-HTC-rh (with hydroxides as basic anions) appears to make little difference in the catalytic activity. We observe little change in activity at 1 h reaction time between Ni-HTC-rh and Ni-HTC-as (Figure S3 in the Supporting Information) or between Ni-HTC-rh prepared without atmospheric exposure and the same catalyst exposed to the atmosphere for 24 h, despite significant differences in basic site concentration measured by benzoic acid titration (Figures S4 and S5 and Table S1 in the Supporting Information), suggesting that  $CO_3^{2-}$  is a strong enough base to serve the catalytic function.

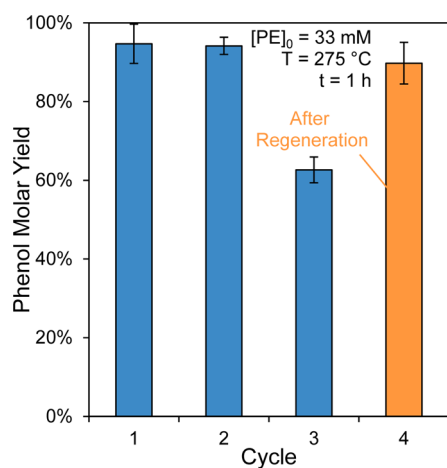
**Recycle and Regeneration.** The critical function of the nitrate anion, along with the general phenomenon that nitrates are converted to other species in reactions in which they participate, suggests that the activity of these materials should be maintained until the nitrate reservoir on the catalyst is depleted and that activity can likely be restored by replenishing the nitrate reservoir. To test this hypothesis, we performed a recycle and regeneration study. As illustrated in Figure 2, the catalyst activity of Ni-HTC-rh is maintained through two cycles, after which activity decreases. The loss in activity is accompanied by a loss of the nitrate-intercalated domains and a partial loss of the HTC structure, as shown by XRD (Figure S6 in the Supporting Information). The partial loss of the HTC structure is not surprising, as loss of interlayer  $H_2O$  and partial dehydroxylation of the brucite layers is known to occur below  $300^\circ C$ .<sup>63</sup> Attempts to restore the HTC structure and  $NO_3^-$  by direct rehydration and direct ion exchange of the used catalyst were unsuccessful, possibly due to a minor amount of carbonaceous material deposited on the catalyst surface. However, calcining the catalyst to fully produce the mixed-oxide state and remove any carbonaceous deposits, followed by rehydration and redeposition of an ethanolic  $Ni(NO_3)_2$  solution, restored catalyst activity. The regeneration protocol is described in the Experimental Section below.

**Effect of Solvent and Substrate on Catalyst Activity.** In previous work, we investigated PE conversion in methyl isobutyl ketone (MIBK) as a representative model system for some organosolv pulping processes.<sup>64–67</sup> However, with a basic catalyst such as HTC, a carbonyl-containing solvent such as MIBK can be deprotonated at the  $\alpha$ -position from the ketone, resulting in side products and solvent degradation. Thus, we were motivated to find an alternative solvent to MIBK for lignin depolymerization. We screened 10 additional solvents, ultimately selecting 3-methyl-3-pentanol (3M3P) as an optimal solvent to maximize catalyst activity and selectivity, solvent stability, substrate solubility, and handling convenience. Further details of the screening are given in Figures S7–S9 in the Supporting Information and the accompanying text.

Similarly, although PE is a convenient lignin model compound due to its ease of synthesis and simplified  $\beta$ -O-4 linkage, realistic lignin substrates will exhibit a more



**Figure 1.** (A) Phenol yield (mol/mol of PE) in the metal-loaded HTC-rh screening study. The horizontal axis shows metal precursor salts. (B) Phenol yield from PE over Ni-HTC-rh catalysts prepared from different precursor salts and a nitrate ion exchanged catalyst prepared from HTC-as. (C) XRD traces for selected catalysts, showing additional peaks from nitrate intercalation. (D) Phenol yield from PE over ion-exchanged HTC catalysts.

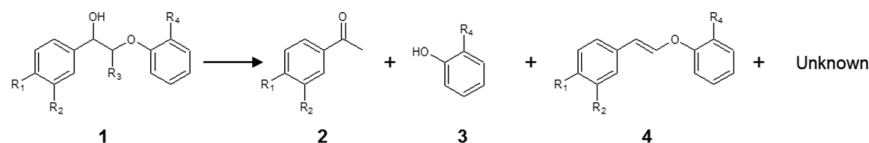


**Figure 2.** Phenol yield (mol/(mol of PE)) during recycling and regeneration of the Ni-HTC-rh catalyst, with regeneration by calcination, rehydration, and redeposition of nitrate after cycle 3. The regeneration protocol includes calcining at  $450 \text{ }^\circ\text{C}$ , rehydrating, and redepositing  $Ni(NO_3)_2$  as an ethanolic solution, as described in the [Experimental Section](#).

heterogeneous suite of linkages and monomers. To further explore the activity of nitrated HTC catalysts, we applied the same reaction conditions used for PE to other lignin model

dimers using 3M3P as solvent. The additional model compounds were selected to represent variations on the  $\beta$ -O-4 linkage and the other predominant linkages found in lignin. The model compounds selected were 1-phenyl-2-phenoxy-1,3-propanediol (PPPD), 1-(3-methoxyphenyl)ethylene glycol- $\beta$ -guaiacyl ether (MGE), veratrylethylene glycol- $\beta$ -guaiacyl ether (VG), guaiacylglycerol- $\beta$ -guaiacyl ether (GG), guaiacylethylene glycol- $\beta$ -guaiacyl ether (GG2), 1,2-diphenylethanol (DPET), 4'-benzyloxy-3'-methoxyacetophenone (BMA), diphenyl ether (DPE), and biphenol (BP).

**$\beta$ -O-4 Dimers.** The model dimers containing a  $\beta$ -O-4 linkage and their reaction products are shown in [Scheme 5](#) and [Table 1](#). The presence of substituents on the rings and inter-ring linkage strongly influences the substrate activity and catalyst effect. In particular, on comparison of PE with PPPD, and of GG2 with GG, it is apparent that the presence of a  $CH_2OH$  group pendant on  $C_\beta$  increases the reactivity of the substrate without any catalyst present and results in a significant fraction of unknown products. Additionally, on comparison of PE with VG and MGE, the presence of  $OCH_3$  substituents on the rings appears to open a second reaction pathway that produces a compound with molecular weight and mass spectrometric fragmentation pattern consistent with a dimeric alkene (product 4 in [Scheme 5](#)), rather than an acyl-aryl ketone and a phenolic compound from the A ring and B ring, respectively. Fragmentation patterns of these compounds are shown in

Scheme 5. Reaction of  $\beta$ -O-4 Model Dimers over HTCTable 1. Reactions of  $\beta$ -O-4 Model Dimers over HTC

name	R1	R2	R3	R4	catalyst	conv of 1	2	3	4 <sup>a</sup>	unknown <sup>b</sup>
PE	H	H	H	H	no cat.	22.0	2.6	3.7	0.0	18.8
					HTC-rh	49.3	24.9	28.5	0.0	22.6
					Ni-HTC-rh	81.9	66.1	72.4	0.0	12.6
					HTC-as(NO <sub>3</sub> )	82.9	73.2	86.2	0.0	3.2
PPPD	H	H	CH <sub>2</sub> OH	H	no cat.	65.5	0.0	0.0	0.0	65.5
					HTC-rh	76.4	12.0	14.9	0.0	62.9
					Ni-HTC-rh	82.0	13.5	31.8	0.0	59.4
					HTC-as(NO <sub>3</sub> )	81.1	14.1	30.9	0.0	58.6
MGE	H	OCH <sub>3</sub>	H	OCH <sub>3</sub>	no cat.	38.7	7.3	12.5	14.4	14.3
					HTC-rh	45.0	30.5	28.5	13.4	2.1
					Ni-HTC-rh	45.7	33.3	24.9	13.1	3.5
					HTC-as(NO <sub>3</sub> )	55.0	47.1	35.5	10.6	3.1
VG	OCH <sub>3</sub>	OCH <sub>3</sub>	H	OCH <sub>3</sub>	no cat.	44.7	5.7	6.4	c	c
					HTC-rh	47.6	8.7	11.6	c	c
					Ni-HTC-rh	47.6	10.2	11.3	c	c
					HTC-as(NO <sub>3</sub> )	47.5	10.7	12.0	c	c
GG	OH	OCH <sub>3</sub>	CH <sub>2</sub> OH	OCH <sub>3</sub>	no cat.	93.8	0.0	55.9	8.0	57.8
					HTC-rh	83.8	0.0	39.2	27.2	37.0
					Ni-HTC-rh	89.7	0.0	35.7	19.0	52.8
					HTC-as(NO <sub>3</sub> )	83.3	0.0	56.2	15.9	39.3
GG2	OH	OCH <sub>3</sub>	H	OCH <sub>3</sub>	no cat.	34.7	0.0	27.4	8.0	12.9
					HTC-rh	90.0	0.0	33.8	27.2	45.9
					Ni-HTC-rh	77.0	0.0	27.4	19.0	44.3
					HTC-as(NO <sub>3</sub> )	89.9	0.0	48.9	15.9	49.5

<sup>a</sup>Alkene quantified as stilbene. <sup>b</sup>Calculated as  $\text{conversion} - 4 - (2 + 3)/2$ . <sup>c</sup>VG decomposes to the alkene in the GC, precluding quantification of that and unknown products.

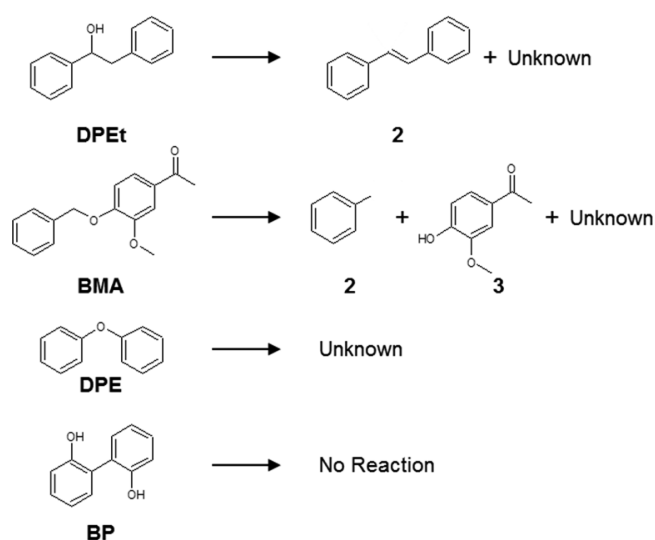
Figures S10–S13 in the Supporting Information. Finally, on comparison of PE with GG2 and PPPD with GG, the presence of a phenolic OH on the A ring appears to preclude the formation of the acyl-aryl ketone, instead forming an unidentified product from the A ring. Although the apparent catalyst activity is not as high for the other substrates as for PE, there is a clear effect on all of the substrates except VG. That is, PPPD and MGE produce significantly more of the A-ring ketone and B-ring phenol in the presence of HTC, while GG and GG2 produce significantly more of the alkene product in the presence of HTC. Additionally, conversion of MGE and GG2 are significantly higher over HTC. In general, the HTC catalysts are able to activate substrates that contain  $\beta$ -O-4 linkages, but the monomer type and yields depend strongly on the substituents of the substrate.

**Other Model Dimers.** We also examined HTC activity for four additional dimers representing other common linkages in lignin. These dimers and their reaction products are shown in Scheme 6 and Table 2. DPET (the model  $\beta$ -1 linkage) readily underwent dehydration to produce *trans*-stilbene over the nitrate-intercalated HTC catalysts, but none of the other

substrates were significantly activated by HTC. BMA was reactive even in the absence of catalyst and produced ~15% yield each of toluene and acetovanillone. DPE showed ~10% conversion, but no reaction products could be identified, and BP showed no detectable conversion. Thus, it appears that the HTC catalysts are not able to activate  $\alpha$ -O-4, 4-O-5, or 5-5 linkages, at least when C<sub>α</sub> on the  $\alpha$ -O-4 substrate has no other substituents. It is worth noting that all of the activated substrates, i.e., the  $\beta$ -O-4 models and DPET, have a benzylic OH group. Thus, it may be the case that the  $\alpha$ -OH group is the key reactive site over the HTC catalysts.

#### Depolymerization of Lignin-Enriched Substrates.

Most importantly, we explored the activity of nitrate-intercalated HTC catalysts toward two process-relevant lignin-enriched streams produced at the pilot scale: a deacetylated, disk-refined, enzymatically hydrolyzed lignin from corn stover (DDE lignin)<sup>68</sup> and a dilute acid pretreated, enzymatically hydrolyzed lignin from corn stover (DAP lignin).<sup>69</sup> The isolation procedures are given in the Experimental Section, and the composition of these lignin-enriched streams is shown in Table 3.

Scheme 6. Reactions of  $\beta$ -1,  $\alpha$ -O-4, 4-O-5, and 5-5 Model Dimers over HTCTable 2. Reactions of  $\beta$ -1,  $\alpha$ -O-4, 4-O-5, and 5-5 Model Dimers over HTC

name	type	catalyst	conv (%)	2	3	unknown
DPEt	$\beta$ -1	no cat.	10.0	1.2		8.8
		HTC-rh	28.3	21.1		7.2
		Ni-HTC-rh	100	100		0.0
		HTC-as(NO <sub>3</sub> )	100	100		0.0
BMA	$\alpha$ -O-4	no cat.	85.0	13.8	12.4	71.9
		HTC-rh	75.7	15.4	16.1	59.9
		Ni-HTC-rh	79.6	14.2	11.7	66.6
		HTC-as(NO <sub>3</sub> )	73.3	14.4	14.1	59.1
DPE	4-O-5	no cat.	7.8			7.8
		HTC-rh	10.0			10.0
		Ni-HTC-rh	12.0			12.0
		HTC-as(NO <sub>3</sub> )	9.9			9.9
BP	5-5	no cat.	0.0			
		HTC-rh	0.0			
		Ni-HTC-rh	0.0			
		HTC-as(NO <sub>3</sub> )	0.0			

Table 3. Compositional Analysis of Lignin-Enriched Streams

substrate	composition (%)						
	lignin	glucan	xylan	galactan	arabinan	acetate	protein
DDE	35.3	25.4	20.8	1.6	3.5	1.1	6.3
DAP	61.3	13.0	1.8	0.0	0.4	0.8	6.0

We evaluated depolymerization of DDE and DAP corn stover lignins in four catalytic scenarios (no catalyst, HTC-rh, Ni-HTC-rh, and HTC-as(NO<sub>3</sub>)) and in two solvents (H<sub>2</sub>O and 3M3P). Despite finding that H<sub>2</sub>O was not a high-performing solvent for  $\beta$ -O-4 bond cleavage in the model dimer PE, we were still interested in exploring aqueous lignin depolymerization over HTC to facilitate integration into upstream and downstream biorefining processes.

**Gel Permeation Chromatography.** When these two lignin streams are subjected to the same reaction conditions as for the

model dimers, significant depolymerization occurs. Some monomeric and dimeric species are produced without catalyst and with HTC-rh, but the fraction is significantly increased with HTC-as(NO<sub>3</sub>) in both 3M3P and H<sub>2</sub>O and with Ni-HTC-rh in water. As shown in Figure 3, the most prominent peaks after acetylation correspond to apparent molecular weights of 200–300 Da. Thus, nitrate-intercalated catalysts are highly active for depolymerization of biomass-derived lignin. For reference,  $M_w$ ,  $M_n$ , and  $M_p$  are reported in Figure S14 in the Supporting Information.

**Yields of Detectable Monomers.** We also attempted to identify and quantify a subset of the monomeric species produced by the HTC catalysts. The main detected monomeric products from both DAP and DDE lignins in H<sub>2</sub>O were phenol, guaiacol, and syringol, with smaller amounts of the corresponding acyl ketones (acetosyringone and acetovanillone) and minute amounts of the corresponding aldehydes (syringaldehyde and vanillin). When the aqueous reaction products were run on HPLC without extraction by dichloromethane (DCM), small amounts of 4-hydroxy-benzaldehyde and 4-hydroxyacetophenone could also be detected. In total, monomer yields detected by GC were 3.5–4.5% without catalyst and ~7% with catalyst, referenced to the lignin mass content in the feedstock, as shown in Figure 4A,B.

In contrast, the major product from both substrates in 3M3P was 4-vinylphenol (4-VP; Figure 4C,D, and Figures S15 and S16 in the Supporting Information), which is produced in 4–7 wt % yields from DDE lignin and 4–5 wt % yields from DAP lignin. Minor products included guaiacol, syringol, 4-ethylphenol, 4-vinylguaiacol, isoeugenol, acetovanillone, and allyl syringol. Total quantified monomer yields over the HTC catalysts were 5–6 wt % from DAP lignin and 7–9 wt % from DDE lignin; the corresponding selectivity to 4-VP was 76–80% from DAP lignin and 60–76% from DDE lignin.

Yields of the detected monomeric products are lower than expected from the GPC traces, especially for the cases with aqueous solvent. The monomers suggested to be present by GPC, but not quantified by GC, could not be conclusively determined. There were no large unidentified peaks on the GC, and standards of several aromatic acids were run on both GC-MS and LC-MS to match retention times and MS fragmentation patterns. Similarly, because the lignin streams under evaluation contain significant fractions of residual carbohydrates, sugar-derived monomeric species, such as 5-hydroxymethyl furfural, furfural, other furan derivatives, and aliphatic acids, were run (Table S2 in the Supporting Information), but could not be matched, by LC.

## DISCUSSION AND CONCLUSIONS

Cost-effective lignin valorization strategies to chemicals and fuels in a biorefinery will rely on the development of cheap, recyclable catalysts. We previously reported that Ni-HTC catalysts are effective for depolymerization of insoluble lignin and active for  $\beta$ -O-4 bond scission in a lignin model compound.<sup>58</sup> Catalysts synthesized from HTC are advantageous because they are heterogeneous, generally nontoxic, and inexpensive. Thus, we were motivated to understand the source of activity and principle of operation for the Ni-HTC catalyst in order to develop a regeneration protocol and improve activity and economics over our initial baseline. The correlation of high catalyst activity with structural changes to the catalyst upon nitrate intercalation suggests that the nitrate is acting heterogeneously. To test this hypothesis, we examined the

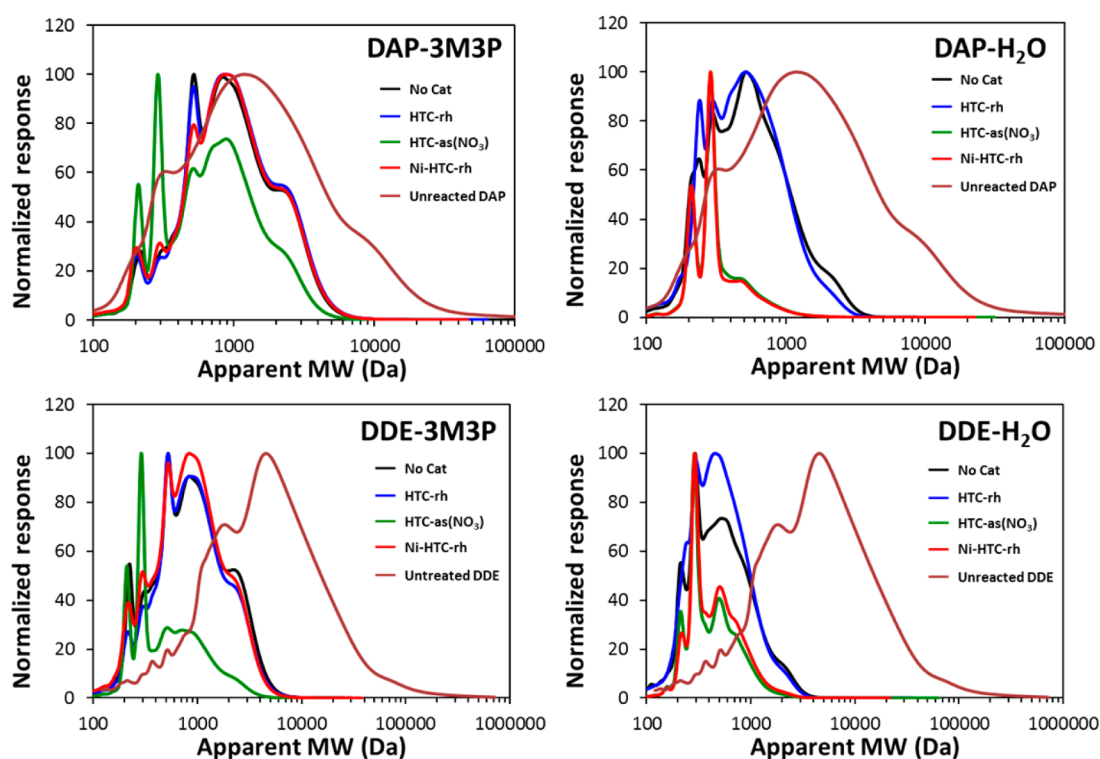


**Figure 3.** GPC traces for the THF-soluble portion of DAP and DDE lignins before and after reaction in 3M3P and H<sub>2</sub>O solvents. Lignins were acetylated for GPC analysis.

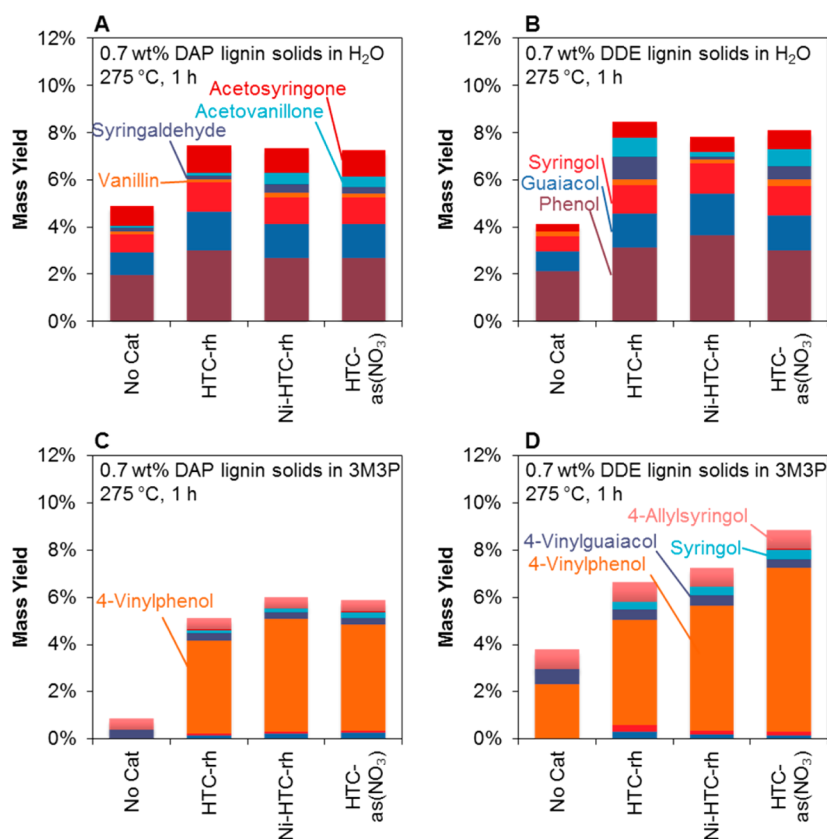


**Figure 4.** Yields of DCM-extracted monomers from DDE and DAP lignins reacted over HTC catalysts in H<sub>2</sub>O solvent (A, B) and yields of monomers over HTC catalysts in 3M3P solvent (C, D).

potential contribution of homogeneous chemistry to our observed results. We performed a hot filtration test to ascertain

if the reaction continues after the catalyst is removed, and control experiments with homogeneous Ni(NO<sub>3</sub>)<sub>2</sub>·6H<sub>2</sub>O,

NaNO<sub>3</sub>, and Na<sub>2</sub>CO<sub>3</sub> to test if the homogeneous anions have activity when not associated with the solid HTC structure. The reaction stops when the catalyst is removed from the solution (Figures S17 and S18 in the Supporting Information), and homogeneous Ni, NO<sub>3</sub><sup>-</sup>, and CO<sub>3</sub><sup>2-</sup> do not show significant catalytic activity (Figure S19 in the Supporting Information). Thus, the nitrate activity is heterogeneous.

There are several possible mechanisms by which heterogeneous nitrate may function:

- increased accessibility to basic sites, due to larger interlayer spacing
- introduction of an easily displaced anion, which allows the substrate access to basic catalytic sites and/or coordination to the metal ions in the brucite layers
- oxidation of PE alcohol to a PE ketone intermediate, which has a lower C<sub>β</sub>-O bond strength
- initiation of a radical mechanism
- nitration of the PE molecule, facilitating decomposition

While we have not conclusively determined the mechanism, we have performed some preliminary experiments that suggest that some of these functions are not active. First, the solely base catalyzed mechanism for PE decomposition is well-known and includes 1-phenylethylene glycol (PhEG) as an intermediate.<sup>70–72</sup> However, when PhEG is used as a starting material with these catalysts, little acetophenone is produced (Figure S20 in the Supporting Information), suggesting that the mechanism is not purely base catalyzed and, hence, easier access to the basic sites is not the only role of the nitrate. Similarly, while the nitrate ion is one of the most easily displaced anions from HTC,<sup>61</sup> if catalyst activity depended on nitrate displacement by a PE molecule, intermediate activity should be observed over the chloride-exchanged HTC, as Cl<sup>-</sup> is easier to displace than CO<sub>3</sub><sup>2-</sup>, but not as easy as NO<sub>3</sub><sup>-</sup>.<sup>61,73,74</sup> Figure 1D shows that the chloride-exchanged catalyst is actually less active than the carbonate form.

Second, if oxidation of PE to PE ketone were part of the reaction pathway, PE ketone should be observable as an intermediate unless it is rapidly consumed. However, kinetic measurements show that PE ketone is never present in significant quantities (Figure S3 in the Supporting Information), and when PE ketone is used as a starting material, conversion after 1 h is only ~50% (Figure S21 in the Supporting Information). The kinetics are not limited by external mass transfer (Figure S22 in the Supporting Information), which, together with the other PE ketone results, suggests that PE ketone is not an intermediate, rapidly consumed or otherwise. Additionally, we observed no significant decrease in activity upon adding the radical quencher BHT to the reaction, suggesting that the primary reaction pathway does not involve radical chemistry (Figure S23 in the Supporting Information).

Finally, the mechanism most consistent with the results involves nitration. While nitration from nitrate typically occurs under conditions much different from those in the current experiments,<sup>75–77</sup> our reaction temperatures may be sufficient to decompose the nitrate into NO and NO<sub>2</sub> species,<sup>78,79</sup> which would be more likely to interact with the substrates. Furthermore, Lindeberg and Walding found that nitration on the B ring of a lignin model increased the reaction rate of base-catalyzed β-O-4 cleavage by more than 3 orders of magnitude and resulted in nitrophenols as reaction intermediates.<sup>80</sup> We reacted 2-nitrophenol, 4-nitrophenol, and 2,4-dinitrophenol

under the same conditions, but no phenol was formed. Thus, ring nitration appears not to be the primary pathway, which leads us to tentatively suggest nitration of the benzylic OH group as a key step in the mechanism. The mechanism will be explored in more detail in subsequent studies.

Another important result of these experiments is that precautions against atmospheric exposure, a concern for basic catalysts originating from HTC,<sup>84–86</sup> appear unnecessary for β-O-4 bond scission in the presence of NO<sub>3</sub><sup>-</sup> anions. Thus, as-synthesized HTC, which is produced commercially, can be used for β-O-4 bond scission after loading with NO<sub>3</sub><sup>-</sup>. Furthermore, we have shown that HTC-based catalysts can be prepared by multiple methods, including simple precipitation–deposition and ion-exchange techniques, both of which are scalable to an industrial level. Additionally, it is possible to directly synthesize NO<sub>3</sub>-HTC,<sup>62</sup> which should also find limited barriers to scale-up.

Regarding the results described for lignin-enriched biorefinery substrates, the formation of 4-VP in 3M3P suggests that the catalyst is also active for ester linkages, as the primary source of 4-VP is likely *p*-coumaric acid. *p*-Coumaric acid is known<sup>81,82</sup> to decarboxylate to 4-VP readily at temperatures below 200 °C, and the decarboxylation is enhanced by basic conditions.<sup>83</sup> Coumarate ester linkages are often considered to be the bridge between lignin and hemicellulose but may also take the place of the analogous alcohol monomer building blocks (Scheme 1), especially in herbaceous biomass. As noted by Ralph, coumarate-type monomers can account for up to 18% of biomass in corn stover, often as pendant groups on S-type lignin.<sup>4</sup> Thus, it may be possible to significantly improve yields of 4-VP and/or *p*-coumaric acid under optimized conditions.

Quantified monomer yields from two process-relevant lignin streams reach 7 wt % in H<sub>2</sub>O solvent, although GPC suggests that actual monomer yields may be much higher. Similarly, in 3M3P, monomer yields, comprised mainly of 4-VP, conservatively reach 5–9 wt %. While these yields are lower than those reported in some other catalytic systems, they are not optimized. However, they are achieved using a catalyst that is inexpensive, easily regenerated, does not require pressurized H<sub>2</sub>, and does not generate high-salt-content wastewater. Furthermore, the selectivity to 4-VP in 3M3P solvent suggests an opportunity to improve yields to 4-VP and/or *p*-coumaric acid, which will facilitate integration of the depolymerization step into downstream upgrading opportunities.<sup>8,87–89</sup>

In summary, HTC-based materials are effective catalysts for lignin depolymerization: namely, for cleavage of β-O-4 bonds and ester linkages. We show here that HTCs containing intercalated NO<sub>3</sub><sup>-</sup> anions increase activity by 2–3-fold for some model compounds but that some accompanying basicity is required for maximum activity. Both the strongly basic OH<sup>-</sup> and the weakly basic CO<sub>3</sub><sup>2-</sup> appear to be active for base catalysis under the conditions studied. Quantified monomer yields from two process-relevant lignin streams are around 7–9 wt % in aqueous solvent and 5–9 wt % in 3M3P. Simple replenishment of the NO<sub>3</sub> “reservoir” on the catalyst and regeneration of the HTC structure from the partially dehydrated state is effective in restoring catalyst activity.

## ■ EXPERIMENTAL SECTION

**Materials.** All materials were used as received. Acetone (HPLC grade), methanol (laboratory grade), diethyl ether (99.5%), NaOH (99%), NaCl (99.9%), hexanes (ACS reagent

grade), ethyl acetate (99.9%), (*R*)-(-)-1,2-diphenylethanol, and methyl isobutyl ketone (MIBK, 4-methyl-2-pentanone, reagent grade) were purchased from Fisher Scientific. Ethanol (200 proof) was purchased from Pharmco-AAPER. 2-Bromoacetophenone (98%), phenol (99%),  $K_2CO_3$  (99%), KI (99%), hydrotalcite (HTC), acetone (HPLC grade), THF (anhydrous), methyl isobutyl ketone (MIBK, HPLC grade),  $NaNO_3$  (99%),  $Ni(NO_3)_2 \cdot 6H_2O$  (19–21% Ni),  $Cr(NO_3)_3 \cdot 9H_2O$  (99%),  $K_2CrO_4$  (99%), NaH (60% in mineral oil), butylated hydroxytoluene (BHT, 99%),  $VCl_2$  (95%),  $Ga(NO_3)_3 \cdot 6H_2O$  (99.5%),  $NiCl_2 \cdot 6H_2O$  (98%),  $Ni(CH_3COO)_2 \cdot 4H_2O$  (98%), 2,2'-biphenol (99%), heptane (99%), *i*-PrOH (99.5%, HPLC grade), acetonitrile (99.8%), 2EH (99+%), diphenyl ether (ReagentPlus, 99%), and 3M3P ( $\geq 99\%$ ) were purchased from Sigma-Aldrich.  $NaBH_4$  (99%),  $Mn(NO_3)_2 \cdot 4H_2O$  (99%),  $Fe(NO_3)_3 \cdot 9H_2O$  (98%),  $CrCl_2$  (97%),  $Cu(NO_3)_2 \cdot 6H_2O$  (99%),  $Zn(NO_3)_2 \cdot 6H_2O$  (99%),  $Ni(HCOO)_2 \cdot 2H_2O$  (98%), and BMA (98%) were purchased from Alfa Aesar.  $MgSO_4$  (99%),  $HNO_3$  (69%), HCl (37%),  $Co(NO_3)_2 \cdot 6H_2O$  (98%),  $Na_2CO_3$  (anhydrous), and toluene (99.8%) were purchased from J. T. Baker.  $VCl_3$  (95%) was purchased from Strem Chemicals. *t*-BuOH (99.5%) was purchased from Acros Organics. GG (97%) was purchased from TCI America. GG2 (purity  $>95\%$  verified by NMR) was purchased from Synthons, Inc.

DDE lignin was produced from 25–50 mm particles of corn stover. The biomass was deacetylated in 0.1 M NaOH (8 wt % total solids) at 80 °C for 2 h, then rinsed with 45 °C water until the pH was 8.5, and dried under flowing air. In some cases, an acid treatment step can be incorporated after deacetylation to prevent microbial growth, but it is not necessary. In those cases, the acid is typically  $H_2SO_4$  at 0.8 wt % concentration (10 wt % with respect to the lignin), and the temperature can range from room temperature to 160 °C for up to 2 h. The resulting material was disk-refined to 1–5 mm particles, but other mechanical refining processes have a similar effect. The refined material was enzymatically hydrolyzed at 15 wt % solids and 50 °C for 72 h in pH 5.1  $NH_4OH$ -citrate buffer using Novozymes CTEC3 (cellulase) and HTEC3 (xylanase) enzymes at 60 mg of protein/g of cellulose and 40 mg protein/g of cellulose, respectively. The lignin content of the starting material was about 15.2 wt %, and of the isolated DDE lignin was 35.3 wt %.

DAP lignin was produced at NREL from corn stover at 8 wt % total solids in 0.8 wt %  $H_2SO_4$  at 160 °C for 10 min and then neutralized to pH 5.1 with NaOH and enzymatically hydrolyzed under the same conditions as for the DDE lignin. The lignin content of the starting material was about 15.2 wt % and of the isolated DAP lignin was 61.3 wt %.

**Model Compound Synthesis. 2-Phenoxy-1-phenylethanol (PE).** 2-Phenoxy-1-phenylethanol (PE) was synthesized in a two-step process as previously described.<sup>58</sup> First, 2-bromoacetophenone (11.94 g, 60 mmol), phenol (7.06 g, 75 mmol),  $K_2CO_3$  (12.30 g, 89 mmol), KI (catalytic), and acetone (250 mL) were heated at reflux overnight, filtered, concentrated, and recrystallized from cold ethanol (250 mL) to give 2-phenoxy-1-phenethanone (PE ketone) in 85% mass yield. Second, PE ketone (1.11 g, 5.2 mmol) was dissolved in methanol (35 mL), and  $NaBH_4$  (0.35 g, 10.4 mmol) was added gradually, after which the mixture was stirred at room temperature for 2 h to reduce the ketone to the alcohol. The reaction mixture was quenched by adding 30 mL of saturated aqueous  $NH_4Cl$ , extracted three times with 50 mL of diethyl ether, washed with 50 mL of saturated NaCl, dried over  $Na_2SO_4$ , and filtered.

Diethyl ether was removed by evaporation to yield PE in 85–90% mass yield.  $^1H$  and  $^{13}C$ -NMR spectra were acquired at 25 °C on a Bruker AVANCE 400 MHz spectrometer equipped with a 5 mm BBO probe. Tetramethylsilane was used as a reference. Data for PE:  $^1H$  NMR ( $CDCl_3$ )  $\delta$  3.90 (1H, s, OH), 4.05 (1H, d,  $J = 2.96$ ,  $H_\beta$ ), 4.07 (1H, s,  $H_\beta$ ), 5.07 (1H, dd,  $J = 4.84$ , 7.00,  $H_\alpha$ ), 6.90–7.45 (10H, m, aromatic H).

**1-(3-Methoxyphenyl) Ethylene Glycol- $\beta$ -guaiacyl Ether (MGE).** To a solution of guaiacol (1.92 g, 15.5 mmol) in acetone (50 mL), 3'-methoxy-2-bromoacetophenone (2.96 g, 12.9 mmol),  $K_2CO_3$  (2.67 g, 19.4 mmol) and KI (0.43 g, 2.58 mmol) were added. The solution was refluxed overnight. The reaction mixture was filtered and the filtrate was concentrated and recrystallized from ethyl acetate/*n*-hexane (1:2, v/v) to give 1-(3-methoxyphenyl)-2-(2-methoxyphenoxy)ethanone (74.7%). To the ethanone derivative (0.98 g, 3.58 mmol) in methanol (10 mL),  $NaBH_4$  (0.27 g, 7.15 mmol) was added gradually. The mixture was stirred at room temperature for 3 h. The reaction mixture was quenched by adding 10 mL of 10% acetic acid, extracted three times with 50 mL of ethyl acetate, washed with brine and dried over  $Na_2SO_4$ . Ethyl acetate was removed by evaporation to yield MGE (99 %). MGE:  $^1H$ -NMR ( $CDCl_3$ ):  $\delta$  3.58 (1H, s, OH), 3.81 (3H, s,  $OCH_3$ ), 3.88 (3H, s,  $OCH_3$ ), 3.97 (1H, t,  $J = 9.6$ ,  $H_\gamma$ ), 3.97 (1H, t,  $J = 9.6$ ,  $H_\gamma$ ), 4.18 (1H, dd,  $J = 3.2$ , 10,  $H_\beta$ ), 3.97 (1H, t,  $J = 9.6$ ,  $H_\gamma$ ), 5.08 (1H, dd, 2.8, 9.2,  $H_\alpha$ ), 6.83–6.99 (8H, m, aromatic H).  $^{13}C$ -NMR ( $CDCl_3$ ):  $\delta$  55.4 ( $OCH_3$ ), 56.1 ( $OCH_3$ ), 72.5 ( $C_\alpha$ ), 76.5 ( $C_\beta$ ), 111.9 ( $C_2$ ), 112.3 ( $C_4$ ), 113.9 ( $C_3'$ ), 116.2 ( $C_6'$ ), 118.8 ( $C_6$ ), 121.3 ( $C_4'$ ), 122.8 ( $C_5'$ ), 129.7 ( $C_5$ ), 141.4 ( $C_1$ ), 148.2 ( $C_1'$ ), 150.3 ( $C_2'$ ), 160.0 ( $C_3$ ).

**Veratryl Ethylene Glycol- $\beta$ -guaiacyl Ether (VG).** To a solution of guaiacol (0.70 g, 5.67 mmol) in acetone (20 mL), 3',4'-dimethoxy-2-bromoacetophenone (1.0 g, 3.86 mmol),  $K_2CO_3$  (0.78 g, 5.67 mmol) and KI (0.062 g, 0.38 mmol) were added. The solution was refluxed overnight. The reaction mixture was filtered. Filtrate was diluted with deionized  $H_2O$  (50 mL) and then extracted two times with ethyl acetate (50 mL). Combined organic layer was washed with brine, dried over  $Na_2SO_4$ , and evaporated, giving a viscous syrup. The crystallization was conducted from ethyl acetate/*n*-hexane (10:1, v/v) to give 1-(3,4-dimethoxyphenyl)-2-(2-methoxyphenoxy)ethanone (78.9 %). To the ethanone derivative (0.92 g, 3.0 mmol) in methanol/ethyl acetate (1:2, v/v, 15 mL),  $NaBH_4$  (0.46 g, 12.1 mmol) was added gradually. The mixture was stirred at room temperature for 2 h. The reaction mixture was quenched by adding 13 mL of 10% acetic acid, extracted three times with 40 mL of ethyl acetate, washed with brine and dried over  $Na_2SO_4$ . Ethyl acetate was removed by evaporation to yield VG (97.5 %). VG:  $^1H$ -NMR ( $CDCl_3$ ):  $\delta$  3.84 (3H, s,  $OCH_3$ ), 3.86 (3H, s,  $OCH_3$ ), 3.88 (3H, s,  $OCH_3$ ), 3.98 (1H, t,  $J = 9.6$ ,  $H_\beta$ ), 4.14 (1H, dd,  $J = 2.8$ , 9.6,  $H_\beta$ ), 5.05 (1H, dd, 2.8, 9.2,  $H_\alpha$ ), 6.83–7.01 (7H, m, aromatic H).  $^{13}C$ -NMR ( $CDCl_3$ ):  $\delta$  55.9 ( $OCH_3$ ), 55.97 ( $OCH_3$ ), 56.04 ( $OCH_3$ ), 72.2 ( $C_\alpha$ ), 76.3 ( $C_\beta$ ), 109.6 ( $C_2$ ), 111.2 ( $C_3'$ ), 112.1 ( $C_5$ ), 115.9 ( $C_6'$ ), 118.7 ( $C_6$ ), 121.2 ( $C_4'$ ), 122.5 ( $C_5'$ ), 132.5 ( $C_1$ ), 148.2 ( $C_1'$ ), 148.9 ( $C_4$ ), 149.2 ( $C_2'$ ), 150.1 ( $C_3$ ).

**1-Phenyl-2-phenoxy-1,3-propanediol (PPPD).** To a solution of 1-phenyl-2-phenoxyethanone (PE-ketone, 1.98 g, 9.33 mmol) in acetone (50 mL), formaldehyde (36 wt % aqueous solution), 0.765 mL, 10 mmol) and  $K_2CO_3$  (0.84 g, 6.08 mmol) were added. The solution was stirred at room temperature for 20 h. After reaction, the reaction mixture was filtered. Solvent in the filtrate was removed. The crude reaction

mixture was purified by column chromatography using 4:1 hexanes:ethyl acetate as eluent. Purified PPPD was recovered in 68% yield. PPPD (Erythro/threo mixture):  $^1\text{H-NMR}$  ( $\text{CDCl}_3$ ):  $\delta$  2.92 (1H, s, OH), 3.56 (1H, dd,  $J = 4.0, 12.4$ ,  $\text{H}_\beta$ ), 3.84 (1H, dd,  $J = 4.0, 12.0$ ,  $\text{H}_\beta$ ), 4.42 (1H, m,  $\text{H}_\beta$ ), 5.04 (1H, d,  $J = 6.4$ ,  $\text{H}_\alpha$ ), 6.96–7.43 (10H, m, aromatic H).  $^{13}\text{C-NMR}$  ( $\text{CDCl}_3$ ):  $\delta$  61.3 ( $\text{C}_\gamma$ ), 74.2 ( $\text{C}_\alpha$ ), 83.2 ( $\text{C}_\beta$ ), 116.8, 122.2, 126.5, 127.1, 128.5, 128.7, 129.8, 129.9, 139.9, 158.3 (Arom-C).  $^1\text{H-NMR}$  spectra of PE, MGE, VG, and PPPD are shown in Figures S24, S25, S26, and S27, respectively.

**Catalyst Preparation.** The base case catalyst was prepared by calcining commercial HTC (HTC-as) at 450 °C for 16 h to generate the mixed-oxide form (HTC-ca). The calcined form was rehydrated by stirring in deionized water for 1.5 h and sonicating in the same water for 5 min to generate the meixnerite form (HTC-rh). A solution of  $\text{Ni}(\text{NO}_3)_2 \cdot 6\text{H}_2\text{O}$  in ethanol was added to give a nominal Ni loading of 5 wt %; the slurry was stirred for 5 min and dried overnight to give Ni-HTC-rh. In this preparation, all calcining, drying, and storage of prepared catalyst were done in an open atmosphere with no effort to exclude  $\text{CO}_2$ . For comparison, uncalcined HTC was washed with hexanes to remove residual carbonaceous material from the manufacturing process and loaded with 5 wt % Ni; this catalyst is labeled Ni-HTC-as. Other metal catalysts were prepared as for Ni-HTC-rh, substituting the appropriate precursor for  $\text{Ni}(\text{NO}_3)_2 \cdot 6\text{H}_2\text{O}$ . Because anhydrous  $\text{VCl}_2$ ,  $\text{VCl}_3$ , and  $\text{CrCl}_2$  were not soluble in ethanol, these were prepared from aqueous solution.

A second set of catalysts was prepared by ion exchange methods, following the general approach of Iyi et al.<sup>73,74</sup> Briefly, a known amount of HTC-as was immersed in a solution of acid (HCl or  $\text{HNO}_3$ ) and sodium salt (NaCl or  $\text{NaNO}_3$ ). The acid concentration was such that the molar ratio  $\text{H}^+:\text{CO}_3^{2-}$  was 2, and the salt concentration was generally >2 M. To obtain an XRD-pure  $\text{Cl}^-$ -form catalyst, two steps with concentrated NaCl were required; the second step did not incorporate acid. From the  $\text{Cl}^-$ -exchanged catalyst, an additional ion exchange was performed with  $\text{NaNO}_3$  to generate a fully nitrate exchanged catalyst.

Two series of catalysts were prepared by varying the time exposed to the atmosphere. For the first set, commercial HTC was calcined in air at 450 °C for 16 h to generate the mixed-oxide form and removed from the furnace hot (~250 °C). This HTC-ca was placed in a round-bottom flask and immediately flushed with  $\text{N}_2$ . Deionized water was added to the flask, and the slurry was stirred for 1 h under flowing  $\text{N}_2$ , the flask was sealed with a rubber septum, and the slurry was sonicated for 5 min. This catalyst was filtered by vacuum filtration under a  $\text{N}_2$  atmosphere and dried overnight under flowing  $\text{N}_2$ . When dry, this catalyst was transferred to an open-top vessel exposed to air. One gram samples were taken periodically from this HTC-rh, placed in glass vials that were then purged with  $\text{N}_2$  and sealed with a rubber septum and Parafilm to study the adsorption of  $\text{CO}_2$  onto the rehydrated form as a function of atmospheric exposure time. These samples are labeled HTC-rh- $x$ h, where  $x$  is the number of hours exposed to the atmosphere.

For the second set, HTC-rh was prepared without exposure to  $\text{CO}_2$  as described above for the first set, and a solution of  $\text{Ni}(\text{NO}_3)_2 \cdot 6\text{H}_2\text{O}$  in ethanol was added to give a nominal Ni loading of 5 wt %. The slurry was stirred for 5 min and dried overnight under flowing  $\text{N}_2$  to give the Ni-HTC. When dry, this catalyst was transferred to an open-top vessel exposed to air. One-gram samples were taken from this Ni-HTC and placed in

glass vials that were then purged with  $\text{N}_2$  and sealed with a rubber septum and Parafilm to study the adsorption of  $\text{CO}_2$  onto the nickel-loaded, rehydrated form as a function of atmospheric exposure time. These samples are labeled Ni-HTC- $x$ h, where  $x$  is the number of hours exposed to the atmosphere.

To understand the role of the anion, Ni-HTC-rh catalysts were prepared with different Ni precursor salts.  $\text{NiCl}_2 \cdot 6\text{H}_2\text{O}$  and  $\text{NiSO}_4 \cdot 6\text{H}_2\text{O}$  were prepared from ethanolic solutions as for the  $\text{Ni}(\text{NO}_3)_2 \cdot 6\text{H}_2\text{O}$  precursor. Due to the low solubility of  $\text{Ni}(\text{HCOO})_2 \cdot 2\text{H}_2\text{O}$  and  $\text{Ni}(\text{CH}_3\text{COO})_2 \cdot 4\text{H}_2\text{O}$  in ethanol, the  $\text{Ni}(\text{HCOO})_2 \cdot 2\text{H}_2\text{O}$  catalyst (NiFm<sub>2</sub>-HTC-rh) was prepared from an aqueous precursor solution and the  $\text{Ni}(\text{CH}_3\text{COO})_2 \cdot 4\text{H}_2\text{O}$  catalyst (NiAc<sub>2</sub>-HTC-rh) was prepared from a methanolic solution.

**Catalyst Screening.** Catalyst activity was evaluated by reacting a solution of 33 mM PE in MIBK over the different catalysts at 275 °C. A 3 mL portion of the PE/MIBK was loaded into stainless steel batch reactors (nominal volume capacity 3 mL), 40 mg of catalyst was added, and the reactors were sealed and weighed. With Ni-HTC catalysts, this loading scheme gives a Ni:PE mass ratio of 0.1. The reactors were then placed in a steel holder inside a wire mesh basket and immersed in a fluidized sand bath (Techne SBL-2D). Reactors were removed from the sand bath at the desired time and quenched in water. After reaction, the reactors were weighed to ensure their mass had not decreased during the reaction and the contents were analyzed by GC-FID and GC-MS as described below. Other model dimers and the lignin streams were run under the same conditions, except that in cases of limited solubility the solid material and 3 mL of solvent were added separately to give the equivalent of a 33 mM concentration (for dimers) or 20 mg of substrate (for lignin).

As the fluid dynamics inside the reactors while in the sand bath were unknown, a separate set of experiments was conducted to evaluate potential mass transfer limitations. In these experiments, the reactors were placed inside a hot, sand-filled cup and the contents stirred at a controlled rate using a Parr 5000 MRS apparatus. From these experiments, an “equivalent minimum stir rate” for the fluidized sand bath could be obtained.

The potential for catalyst leaching and homogeneous chemistry was evaluated by running the reaction with PE with inline gas filters as reaction vessels, which were reacted with controlled orientation and flipped at a certain reaction time to hot-filter the catalyst from the reaction solution. These reactors contain a cup-shaped 0.5  $\mu\text{m}$  filter basket that could effectively retain catalyst particles while allowing hot solvent to pass through. Due to the potential for the gas-phase reaction of PE with the separated catalyst, these reactors were flipped while hot to filter the catalyst from the solution, the reaction mixtures were quenched, and the catalyst was physically removed from the reactor. The reaction solution was then allowed to react further in the absence of catalyst. Although these reactors had a nominal volume of 12 mL, the heating curves for these reactors were similar to those for the 3 mL reactors, generally reaching the reaction temperature (275 °C) from room temperature within 7 min.

**Catalyst Recycle and Regeneration.** For recycle studies, larger Parr batch reactors (Parr Series 5000 Multiple Reactor System) were used to more efficiently generate sufficient catalyst for characterization after each reaction cycle. These reactions were scaled up by a factor of 10 from those for the 3

mL reactors, and the contents were stirred at 400 rpm. After each reaction cycle, the catalyst from each reactor was combined to produce a pool of catalyst samples from which samples were withdrawn for characterization; the remaining catalyst was distributed to reactors for the next reaction cycle. For catalyst regeneration, the spent catalyst was calcined for 16 h at 450 °C and then rehydrated and reloaded with an ethanolic solution of Ni(NO<sub>3</sub>)<sub>2</sub> by the same procedure used to generate fresh Ni-HTC-rh.

**Product Analysis.** For dimers except GG, GG2, PPPD, and VG, starting materials and reaction products were analyzed by GC-FID and GC-MS on an HP-5MS capillary column. For GC-FID, the injection volume was 5 μL, the split ratio was 8:1, and the oven program was 100 °C for 3 min, ramp at 20 °C/min to 160 °C, hold for 1.5 min, ramp at 20 °C/min to 250 °C, and hold for 4.3 min. For GC-MS, the column was the same, the injection volume was 1 μL, the split ratio was 25:1, and the oven program was 100 °C for 1 min, ramp at 10 °C/min to 114 °C, hold for 0 min, ramp at 20 °C/min to 160 °C, hold for 1.5 min, ramp at 20 °C/min to 250 °C, and hold for 4.3 min.

For benzoic acid titration experiments, the GC column was the same as above, the injection volume was 1 μL, the system was operated as splitless with the purge valve open at 0.2 min, and the oven program was the same as for GC-FID analysis above.

For DPE, DPET, BP, and BMA, a second method was developed. The method was the same as the GC-MS method described above, except the oven program was 35 °C for 3.5 min, ramp at 10 °C/min to 114 °C, hold for 0 min, ramp at 20 °C/min to 160 °C, hold for 1.5 min, ramp at 20 °C/min to 250 °C, and hold for 4.3 min.

For GG, GG2, PPPD, and VG, the starting material was quantified by HPLC, and products were quantified by GC-FID. For GC analysis, the injection volume was 1 μL, the split ratio was 10:1, the system was operated under constant flow mode of 1 mL/min, and the oven program was 50 °C for 1 min, ramp at 10 °C/min to 250 °C, hold for 0 min, ramp at 25 °C/min to 300 °C, and hold for 5 min.

For HPLC, analysis of samples was performed on an Agilent 1100 LC system equipped with a G1315B diode array detector (DAD) and an Ion Trap SL (Agilent Technologies, Palo Alto, CA) mass spectrometer (MS) with in-line electrospray ionization (ESI). Each sample was injected undiluted at a volume of 50 μL into the LC/MS system.

Phenolic standard compounds were separated using reverse-phase chromatography on an YMC C30 Carotenoid 0.3 μm, 4.6 × 150 mm column (YMC America, Allentown, PA). The chromatography consisted of a solvent regime of water modified with 0.03% formic acid (eluent A) and 9:1 acetonitrile and water also modified with 0.03% formic acid (eluent B) at a constant oven temperature of 30 °C and a solvent flow rate of 0.7 mL min<sup>-1</sup>, with a gradient as follows: 0–3 min, 0% B; 16 min, 7% B; 21 min, 8.5% B; 34 min, 10% B; 46 min, 25% B; 51–54 min, 30% B; 61 min, 50% B; and last 64–75 min, 100% B before equilibrium.

Flow from the HPLC-DAD was directly routed to the ESI-MS ion trap. The DAD was used to monitor chromatography at 210 nm for quantitation and a direct comparison to MS for identification data. Source and ion trap conditions were calibrated with Agilent ESI-T tuning mix (P/N:G2431A), while tuning parameters were optimized under negative ion mode by direct infusion of standards for major contributing compounds. MS and MS/MS tuned parameters are as follows:

smart parameter setting with target mass set to 165 Da, compound stability 10%, trap drive 50%, capillary at 3500 V, fragmentation amplitude of 0.75 V with a 30–200% ramped voltage implemented for 50 ms, and an isolation width of *m/z* 2 (He collision gas). The ESI nebulizer gas was set to 60 psi, with a dry gas flow of 11 L min<sup>-1</sup> held at 350 °C. MS scans and precursor isolation–fragmentation scans were performed across the range of 40–350 Da. This program was used to identify monomers in lignin solutions and to quantify both identified monomers and the model dimer GG.

**Gel Permeation Chromatography (GPC) Analysis.** Each substrate and reaction product (20 mg) was acetylated in a mixture of pyridine (0.5 mL) and acetic anhydride (0.5 mL) at 40 °C for 24 h with stirring. The reaction was terminated by addition of methanol (0.2 mL). The acetylation solvents were then evaporated from the samples at room temperature under a stream of nitrogen gas. Addition of methanol and nitrogen flushing were repeated until the vapors from pyridine and acetic anhydride had dissipated. The samples were further dried in a vacuum oven at 40 °C overnight. The dried, acetylated lignin samples were dissolved in tetrahydrofuran (THF, Baker HPLC grade). The dissolved samples were filtered (0.45 μm nylon membrane syringe filters) before GPC analysis. The acetylated samples were completely soluble in THF. GPC analysis was performed using an Agilent HPLC with 3 GPC columns (Agilent, PLgel, 300 × 7.5 mm) packed with polystyrene–divinylbenzene copolymer gel (10 μm beads) having nominal pore diameters of 10<sup>4</sup>, 10<sup>3</sup>, and 50 Å. The eluent was THF and the flow rate 1.0 mL/min. An injection volume of 25 μL was used. The HPLC was attached to a diode array detector measuring absorbance at 260 nm (bandwidth 80 nm). Retention time was converted into molecular weight (MW) by applying a calibration curve established using polystyrene standards of known molecular weight (1 × 10<sup>6</sup> to 580 Da) plus toluene (92 Da).

**Catalyst Characterization.** Basic sites were quantified by benzoic acid titration using a modified procedure of Parida and Das.<sup>90</sup> Briefly, 0.1 g of catalyst was stirred for 1.5 h in a solution of benzoic acid in hexane, with benzoic acid concentrations ranging from 0.5 to 50 mM. A time of 1.5 h was found to be sufficient for equilibration of adsorption. The change in benzoic acid concentration was measured by GC-FID, and the number of basic sites was determined from the intercept of the linearized Langmuir equation

$$\frac{C}{x} = \frac{1}{\alpha x_m} + \frac{C}{x_m}$$

where *C* is the concentration of benzoic acid in solution (mol/L), *x* is the amount of benzoic acid adsorbed (mol/g<sub>cat</sub>), *x<sub>m</sub>* is the number of basic sites (mol/g<sub>cat</sub>), and *α* is a constant.

Catalysts were also characterized by XRD, ICP, and N<sub>2</sub> physisorption. XRD was performed on a Rigaku Ultima IV X-ray diffraction system using Cu Kα radiation, with operating voltage and current of 40 kV and 44 mA, respectively, scan speed of 5°/min, and point spacing of 0.02°. N<sub>2</sub> physisorption was carried out with a Quantichrome Quantisorb SI four-station instrument, with outgassing at 110 °C for 2 h before analysis, and an equilibration time of 30 s for both adsorption and desorption branches. ICP analysis was conducted on a Spectro Acros FHS12 instrument at a plasma power of 1425 W. Ni was analyzed using the 231.6 nm line.

## ■ ASSOCIATED CONTENT

## ■ Supporting Information

The Supporting Information is available free of charge on the ACS Publications website at DOI: 10.1021/acscatal.5b02062.

Accompanying conversion and yield data for Figure 1, experimental data of reactions with homogeneous catalysts, radical inhibitors, varying basic site concentrations, and nitrite-intercalated HTC, correlations of phenol yield with solvent parameters, conversions and yields from BMA, DPE, and PhEG, identification of 4-VP, monomer candidates not detected by GC, stir rate experiments, kinetic measurements, XRD traces of selected HTC catalysts, nitrate ester decomposition pathways, and catalyst characterization data (PDF)

## ■ AUTHOR INFORMATION

## Corresponding Authors

\*M.J.B.: fax, +01-303-384-6363; tel, +01-303-384-7806; e-mail, [mary.biddy@nrel.gov](mailto:mary.biddy@nrel.gov).

\*G.T.B.: e-mail, [gregg.beckham@nrel.gov](mailto:gregg.beckham@nrel.gov).

## Notes

The authors declare no competing financial interest.

## ■ ACKNOWLEDGMENTS

This work was funded by NREL CRADA 13-513 with Shell Global Solutions, Inc., and by the U.S. Department of Energy Bioenergy Technologies Office. The authors are grateful to Dr. Steven Chmely for synthesis of deuterated PE, to Kelsey Ramirez for assistance with HPLC analysis, to Melvin Tucker, Michael Resch, Xiaowen Chen, and Erik Kuhn for preparation of lignin substrates (DDE and DAP), and to Seonah Kim and Roberto Rinaldi for discussions regarding potential mechanisms.

## ■ REFERENCES

- Zakzeski, J.; Bruijninx, P. C. A.; Jongerius, A. L.; Weckhuysen, B. M. *Chem. Rev.* **2010**, *110*, 3552–3599.
- Ragauskas, A. J.; Beckham, G. T.; Biddy, M. J.; Chandra, R.; Chen, F.; Davis, M. F.; Davison, B. H.; Dixon, R. A.; Gilna, P.; Keller, M.; Langan, P.; Naskar, A. K.; Saddler, J. N.; Tschaplinski, T. J.; Tuskan, G. A.; Wyman, C. E. *Science* **2014**, *344*, 1246843.
- Boerjan, W.; Ralph, J.; Baucher, M. *Annu. Rev. Plant Biol.* **2003**, *54*, 519–546.
- Ralph, J. *Phytochem. Rev.* **2010**, *9*, 65–83.
- Azadi, P.; Inderwildi, O. R.; Farnood, R.; King, D. A. *Renewable Sustainable Energy Rev.* **2013**, *21*, 506–523.
- Parthasarathi, R.; Romero, R. A.; Redondo, A.; Gnanakaran, S. *J. Phys. Chem. Lett.* **2011**, *2*, 2660–2666.
- Kim, S.; Chmely, S. C.; Nimlos, M. R.; Bomble, Y. J.; Foust, T. D.; Paton, R. S.; Beckham, G. T. *J. Phys. Chem. Lett.* **2011**, *2*, 2846–2852.
- Linger, J. G.; Vardon, D. R.; Guarnieri, M. T.; Karp, E. M.; Hunsinger, G. B.; Franden, M. A.; Johnson, C. W.; Chupka, G.; Strathmann, T. J.; Pienkos, P. T. *Proc. Natl. Acad. Sci. U. S. A.* **2014**, *111*, 12013–12018.
- Chundawat, S. P. S.; Beckham, G. T.; Himmel, M. E.; Dale, B. E. *Annu. Rev. Chem. Biomol. Eng.* **2011**, *2*, 121–145.
- Himmel, M. E.; Ding, S.-Y.; Johnson, D. K.; Adney, W. S.; Nimlos, M. R.; Brady, J. W.; Foust, T. D. *Science* **2007**, *315*, 804–807.
- Davis, R.; Tao, L.; Tan, E.; Biddy, M.; Beckham, G.; Scarlata, C.; Jacobson, J.; Cafferty, K.; Ross, J.; and Lukas, J. Process design and economics for the conversion of lignocellulosic biomass to hydrocarbons: Dilute-acid and enzymatic Deconstruction of biomass to sugars and biological conversion of Sugars to Hydrocarbons; National

Renewable Energy Laboratory (NREL): Golden, CO, 2013; No. NREL/TP-5100-60223.

- Wang, X.; Rinaldi, R. *ChemSusChem* **2012**, *5*, 1455–1466.
- Zaheer, M.; Hermannsdörfer, J.; Kretschmer, W. P.; Motz, G.; Kempe, R. *ChemCatChem* **2014**, *6*, 91–95.
- Song, Q.; Wang, F.; Xu, J. *Chem. Commun.* **2012**, *48*, 7019–7021.
- He, J.; Zhao, C.; Lercher, J. A. *J. Am. Chem. Soc.* **2012**, *134*, 20768–20775.
- He, J.; Zhao, C.; Mei, D.; Lercher, J. A. *J. Catal.* **2014**, *309*, 280–290.
- Harris, E. E.; D'Ianni, J.; Adkins, H. *J. Am. Chem. Soc.* **1938**, *60*, 1467–1470.
- Pepper, J. M.; Hibbert, H. *J. Am. Chem. Soc.* **1948**, *70*, 67–71.
- Brewer, C. P.; Cooke, L. M.; Hibbert, H. *J. Am. Chem. Soc.* **1948**, *70*, 57–59.
- Van den Bosch, S.; Schutyser, W.; Vanholme, R.; Driessen, T.; Koelewijn, S.-F.; Renders, T.; De Meester, B.; Huijgen, W.; Dehaen, W.; Courtin, C. *Energy Environ. Sci.* **2015**, *8*, 1748–1763.
- Parsell, T.; Yohe, S.; Degenstein, J.; Jarrell, T.; Klein, I.; Gencer, E.; Hewetson, B.; Hurt, M.; Kim, J. I.; Choudhari, H.; Saha, B.; Meilan, R.; Mosier, N.; Ribeiro, F.; Delgass, W. N.; Chapple, C.; Kenttamaa, H. I.; Agrawal, R.; Abu-Omar, M. M. *Green Chem.* **2015**, *17*, 1492–1499.
- Galkin, M. V.; Sawadjoon, S.; Rohde, V.; Dawange, M.; Samec, J. S. M. *ChemCatChem* **2014**, *6*, 179–184.
- Song, Q.; Wang, F.; Cai, J.; Wang, Y.; Zhang, J.; Yu, W.; Xu, J. *Energy Environ. Sci.* **2013**, *6*, 994–1007.
- Wang, X.; Rinaldi, R. *Angew. Chem., Int. Ed.* **2013**, *52*, 11499–11503.
- Klein, I.; Saha, B.; Abu-Omar, M. M. *Catal. Sci. Technol.* **2015**, *5*, 3242–3245.
- Zhang, J.; Deng, H.; Lin, L. *Molecules* **2009**, *14*, 2747–2757.
- Sales, F. G.; Maranhão, L. C. A.; Filho, N. M. L.; Abreu, C. A. M. *Chem. Eng. Sci.* **2007**, *62*, 5386–5391.
- Crestini, C.; Pro, P.; Neri, V.; Saladino, R. *Bioorg. Med. Chem.* **2005**, *13*, 2569–2578.
- Crestini, C.; Caponi, M. C.; Argyropoulos, D. S.; Saladino, R. *Bioorg. Med. Chem.* **2006**, *14*, 5292–5302.
- Biannic, B.; Bozell, J. J. *Org. Lett.* **2013**, *15*, 2730–2733.
- Lu, F.; Ralph, J. J. *Agric. Food Chem.* **1997**, *45*, 4655–4660.
- Partenheimer, W. *Adv. Synth. Catal.* **2009**, *351*, 456–466.
- Nichols, J. M.; Bishop, L. M.; Bergman, R. G.; Ellman, J. A. *J. Am. Chem. Soc.* **2010**, *132*, 12554–12555.
- vom Stein, T.; Weigand, T.; Merckens, C.; Klankermayer, J.; Leitner, W. *ChemCatChem* **2013**, *5*, 439–441.
- Nagy, M.; David, K.; Britovsek, G. J. P.; Ragauskas, A. J. *Holzforchung* **2009**, *63*, 513–520.
- Chen; Capanema, E. A.; Gracz, H. S. *J. Agric. Food Chem.* **2003**, *51*, 1932–1941.
- Son, S.; Toste, F. D. *Angew. Chem., Int. Ed.* **2010**, *49*, 3791–3794.
- Sedai, B.; Díaz-Urrutia, C.; Baker, R. T.; Wu, R.; Silks, L. A. P.; Hanson, S. K. *ACS Catal.* **2013**, *3*, 3111–3122.
- Harms, R. G.; Markovits, I. I. E.; Drees, M.; Herrmann, h. c. m. W. A.; Cokoja, M.; Kühn, F. E. *ChemSusChem* **2014**, *7*, 429–434.
- Nguyen, J. D.; Matsuura, B. S.; Stephenson, C. R. J. *J. Am. Chem. Soc.* **2014**, *136*, 1218–1221.
- Chmely, S. C.; Kim, S.; Ciesielski, P. N.; Jiménez-Osés, G.; Paton, R. S.; Beckham, G. T. *ACS Catal.* **2013**, *3*, 963–974.
- Gao, Y.; Zhang, J.; Chen, X.; Ma, D.; Yan, N. *ChemPlusChem* **2014**, *79*, 825–834.
- Rahimi, A.; Azarpira, A.; Kim, H.; Ralph, J.; Stahl, S. S. *J. Am. Chem. Soc.* **2013**, *135*, 6415–6418.
- Shabtai, J.; Zmierczak, W., and Chornet, E. Conversion of lignin to reformulated gasoline compositions. 1. Basic processing scheme. *Proceedings of the 3rd Biomass Conference of the Americas*, Montreal, Canada; Elsevier: Amsterdam, 1997; pp 1037–1040.
- Shabtai, J.; Zmierczak, W., Chornet, E., and Johnson, D. K. Conversion of lignin. 2. Production of high-octane fuel additives.

*Preprints of the Symposium-American Chemical Society, Division of Fuel Chemistry*; American Chemical Society, Division of Fuel Chemistry: Washington, DC, 1999; pp 267–272.

(46) Shabtai, J.; Zmierczak, W.; Chornet, E., and Johnson, D. K. Conversion of lignin. 2. Production of high-octane fuel additives. *Abstracts of Papers*, 217th ACS National Meeting, Anaheim, CA; American Chemical Society: Washington, DC, 1999; pp. FUEL-056.

(47) Shabtai, J.; Zmierczak, W.; Kadangode, S.; Chornet, E., and Johnson, D. K. Lignin conversion to high-octane fuel additives. *Biomass: A Growth Opportunity in Green Energy and Value-Added Products*, Proceedings of the 4th Biomass Conference of the Americas, Oakland, CA; Elsevier Science: Amsterdam, 1999; pp 811–818.

(48) Shabtai, J. S.; Zmierczak, W. W.; Chornet, E. U.S. Patent US 09/136,336, 1999.

(49) Shabtai, J. S.; Zmierczak, W. W.; Chornet, E. U.S. Patent US 09/376,864, 2001.

(50) Shabtai, J.; Zmierczak, W.; Chornet, E.; Johnson, D. U.S. Patent US 09/972,461, 2003.

(51) Roberts, V. M.; Stein, V.; Reiner, T.; Lemonidou, A.; Li, X.; Lercher, J. A. *Chem. - Eur. J.* **2011**, *17*, 5939–5948.

(52) Miller, J. E.; Evans, L.; Littlewolf, A.; Trudell, D. E. *Fuel* **1999**, *78*, 1363–1366.

(53) Vigneault, A.; Johnson, D. K.; Chornet, E. *Can. J. Chem. Eng.* **2007**, *85*, 906–916.

(54) Barta, K.; Matson, T. D.; Fettig, M. L.; Scott, S. L.; Iretskii, A. V.; Ford, P. C. *Green Chem.* **2010**, *12*, 1640–1647.

(55) Matson, T. D.; Barta, K.; Iretskii, A. V.; Ford, P. C. *J. Am. Chem. Soc.* **2011**, *133*, 14090–14097.

(56) Barta, K.; Warner, G. R.; Beach, E. S.; Anastas, P. T. *Green Chem.* **2014**, *16*, 191–196.

(57) Warner, G.; Hansen, T. S.; Riisager, A.; Beach, E. S.; Barta, K.; Anastas, P. T. *Bioresour. Technol.* **2014**, *161*, 78–83.

(58) Sturgeon, M. R.; O'Brien, M. H.; Ciesielski, P. N.; Katahira, R.; Kruger, J. S.; Chmely, S. C.; Hamlin, J.; Lawrence, K.; Hunsinger, G. B.; Foust, T. D.; Baldwin, R. M.; Bidy, M. J.; Beckham, G. T. *Green Chem.* **2014**, *16*, 824–835.

(59) Mills, S. J.; Christy, A. G.; Génin, J.-M. R.; Kameda, T.; Colombo, F. *Mineral. Mag.* **2012**, *76*, 1289–1336.

(60) Debecker, D. P.; Gaigneaux, E. M.; Busca, G. *Chem. - Eur. J.* **2009**, *15*, 3920–3935.

(61) Miyata, S. *Clays Clay Miner.* **1983**, *31*, 305–311.

(62) Bontchev, R. P.; Liu, S.; Krumhansl, J. L.; Voigt, J.; Nenoff, T. *M. Chem. Mater.* **2003**, *15*, 3669–3675.

(63) Zhang, J.; Xu, Y. F.; Qian, G.; Xu, Z. P.; Chen, C.; Liu, Q. *J. Phys. Chem. C* **2010**, *114*, 10768–10774.

(64) Katahira, R.; Mittal, A.; McKinney, K.; Ciesielski, P. N.; Donohoe, B. S.; Black, S. K.; Johnson, D. K.; Bidy, M. J.; Beckham, G. T. *ACS Sustainable Chem. Eng.* **2014**, *2*, 1364–1376.

(65) Bozell, J. J.; Black, S. K.; Myers, M.; Cahill, D.; Miller, W. P.; Park, S. *Biomass Bioenergy* **2011**, *35*, 4197–4208.

(66) Bozell, J. J.; O'Lenick, C.; Warwick, S. J. *Agric. Food Chem.* **2011**, *59*, 9232–9242.

(67) Resch, M. G.; Donohoe, B. S.; Ciesielski, P. N.; Nill, J. E.; Magnusson, L.; Himmel, M. E.; Mittal, A.; Katahira, R.; Bidy, M. J.; Beckham, G. T. *ACS Sustainable Chem. Eng.* **2014**, *2*, 1377–1387.

(68) Chen, X.; Shekuro, J.; Pschorn, T.; Sabourin, M.; Tao, L.; Elander, R.; Park, S.; Jennings, E.; Nelson, R.; Trass, O. *Biotechnol. Biofuels* **2014**, *7*, 98.

(69) Chen, X.; Shekuro, J.; Franden, M. A.; Wang, W.; Zhang, M.; Kuhn, E.; Johnson, D. K.; Tucker, M. P. *Biotechnol. Biofuels* **2012**, *5*, 8.

(70) Gierer, J.; Kunze, I. *Acta Chem. Scand.* **1961**, *15*, 803–807.

(71) Gierer, J.; Norén, I. *Acta Chem. Scand.* **1962**, *16*, 1976–1988.

(72) Huo, W.; Li, W.; Zhang, M.; Fan, W.; Chang, H.-m.; Jameel, H. *Catal. Lett.* **2014**, *144*, 1159–1163.

(73) Iyi, N.; Matsumoto, T.; Kaneko, Y.; Kitamura, K. *Chem. Mater.* **2004**, *16*, 2926–2932.

(74) Iyi, N.; Okamoto, K.; Kaneko, Y.; Matsumoto, T. *Chem. Lett.* **2005**, *34*, 932–933.

(75) Sergeeva, L. L.; Shorygina, N. N. *Bull. Acad. Sci. USSR, Div. Chem. Sci.* **1965**, *14*, 1590–1595.

(76) Borsche, W. *Ber. Dtsch. Chem. Ges.* **1917**, *50*, 1339–1355.

(77) Chuksanova, A. A.; Sergeeva, L. L.; Shorygina, N. N. *Bull. Acad. Sci. USSR, Div. Chem. Sci.* **1959**, *8*, 2114–2119.

(78) Stern, K. H. *J. Phys. Chem. Ref. Data* **1972**, *1*, 747–772.

(79) Cseri, T.; Békássy, S.; Kenessey, G.; Liptay, G.; Figueras, F. *Thermochim. Acta* **1996**, *288*, 137–154.

(80) Lindeberg, O.; Walding, J. *Tappi J.* **1987**, *70*, 119–123.

(81) de Groot, M.; Buma, W. J. *J. Phys. Chem. A* **2005**, *109*, 6135–6136.

(82) Terpinč, P.; Polak, T.; Šegatin, N.; Hanzlowsky, A.; Ulrih, N. P.; Abramovič, H. *Food Chem.* **2011**, *128*, 62–69.

(83) Nomura, E.; Hosoda, A.; Mori, H.; Taniguchi, H. *Green Chem.* **2005**, *7*, 863–866.

(84) Abelló, S.; Vijaya-Shankar, D.; Pérez-Ramírez, J. *Appl. Catal., A* **2008**, *342*, 119–125.

(85) Debecker, D. P.; Gaigneaux, E. M.; Busca, G. *Chem. - Eur. J.* **2009**, *15*, 3920–3935.

(86) Di Cosimo, J. L.; Diez, V. K.; Xu, M.; Iglesia, E.; Apesteguía, C. *R. J. Catal.* **1998**, *178*, 499–510.

(87) Vardon, D. R.; Franden, M. A.; Johnson, C. W.; Karp, E. M.; Guarnieri, M. T.; Linger, J. G.; Salm, M. J.; Strathmann, T. J.; Beckham, G. T. *Energy Environ. Sci.* **2015**, *8*, 617–628.

(88) Johnson, C. W.; Beckham, G. T. *Metab. Eng.* **2015**, *28*, 240–247.

(89) Salvachúa, D.; Karp, E. M.; Nimlos, C. T.; Vardon, D. R.; Beckham, G. T. *Green Chem.* **2015**, *17*, 4951–4967.

(90) Parida, K.; Das, J. J. *Mol. Catal. A: Chem.* **2000**, *151*, 185–192.